THE JOURNAL OF BIOLOGICAL CHEMISTRY VOL. 291, NO. 33, pp. 17165–17177, August 12, 2016

Identification of Plant-derived Alkaloids with Therapeutic Potential for Myotonic Dystrophy Type I*

Received for publication, December 14, 2015, and in revised form, June 10, 2016 Published, JBC Papers in Press, June 13, 2016, DOI 10.1074/jbc.M115.710616

Ruben Herrendorff[‡], Maria Teresa Faleschini[§1], Adeline Stiefvater[‡], Beat Erne[‡], Tatiana Wiktorowicz[‡], Frances Kern[‡], Matthias Hamburger[§], Olivier Potterat[§], Jochen Kinter[‡2], and Michael Sinnreich[‡3]

From the [‡]Neuromuscular Research Group, Departments of Neurology and Biomedicine, University Hospital Basel, Klingelbergstrasse 50, 4056 Basel, Switzerland and the [§]Division of Pharmaceutical Biology, Department of Pharmaceutical Sciences, University of Basel, Klingelbergstrasse 50, 4056 Basel, Switzerland

Myotonic dystrophy type I (DM1) is a disabling neuromuscular disease with no causal treatment available. This disease is caused by expanded CTG trinucleotide repeats in the 3′ UTR of the dystrophia myotonica protein kinase gene. On the RNA level, expanded $(CUG)_n$ repeats form hairpin structures that sequester splicing factors such as muscleblind-like 1 (MBNL1). Lack of available MBNL1 leads to misregulated alternative splicing of many target pre-mRNAs, leading to the multisystemic symptoms in DM1. Many studies aiming to identify small molecules that target the $(CUG)_n$-MBNL1 complex focused on synthetic molecules. In an effort to identify new small molecules that liberate sequestered MBNL1 from $(CUG)_n$ RNA, we focused specifically on small molecules of natural origin. Natural products remain an important source for drugs and play a significant role in providing novel leads and pharmacophores for medicinal chemistry. In a new DM1 mechanism-based biochemical assay, we screened a collection of isolated natural compounds and a library of over 2100 extracts from plants and fungal strains. HPLC-based activity profiling in combination with spectroscopic methods were used to identify the active principles in the extracts. The bioactivity of the identified compounds was investigated in a human cell model and in a mouse model of DM1. We identified several alkaloids, including the β-carboline harmine and the isoquinoline berberine, that ameliorated certain aspects of the DM1 pathology in these models. Alkaloids as a compound class may have potential for drug discovery in other RNA-mediated diseases.

Myotonic dystrophy type I (DM1)[4] is the most common muscular dystrophy in the adult population, with a relatively high prevalence of about 1:8000 (1). This autosomal dominantly inherited disease affects multiple organs, most prominently the skeletal muscle, with wasting, weakness, and an inability to relax (myotonia) (1). Currently, there is no effective treatment for this disabling disease. The pathomechanism of DM1 is linked to a CTG_n expansion in the 3′ UTR of the dystrophia myotonica protein kinase (*DMPK*) gene (2, 3), leading to a toxic gain-of-function RNA (4, 5). The mutant DMPK transcript is entrapped within nuclei of affected cells, where it forms aggregates (foci) with splicing factors such as muscleblind-like 1 (MBNL1) (6, 7). Bound to mutant DMPK $(CUG)_n$ RNA, MBNL1 is no longer available for correct splicing of its target pre-mRNAs (8, 9). Thus, the splicing of a multitude of pre-mRNAs is misregulated, including the skeletal muscle chloride channel (*CLCN1*), the insulin receptor (*INSR*), sarcoplasmic/endoplasmic reticulum Ca^{2+} ATPase 1 (*SERCA1*), and cardiac troponin T type 2 (*TNNT2*) pre-mRNA (10–16). Interestingly, the missplicing of some pre-mRNAs can be linked directly to a certain disease symptom, *e.g.* myotonia in the case of the CLCN1 pre-mRNA. MBNL1 sequestration by $(CUG)_n$ RNA causes inclusion of alternative exon 7a, leading to a shift in the open reading frame and to premature termination of translation (12, 13). As a result, functional CLCN1 protein is decreased, which leads to the myotonia characteristic of DM1 (17).

To date, most therapeutic strategies toward DM1 focused either on the development of agents degrading the toxic RNA or blocking its pathogenic interaction with proteins; these strategies are reviewed in Ref. 18. Antisense oligonucleotides targeting the DMPK-$(CUG)_n$ transcripts (5, 19) and viral overexpression of MBNL1 (20) have been shown to reverse the toxic RNA effect *in vitro* and *in vivo*. Compared with the antisense oligonucleotide and gene therapy approaches, an advantage of a suitable small molecule is its potential to penetrate all tissues affected in DM1 patients and its potential oral bioavailability. A variety of small molecules have been described that inhibit the $(CUG)_n$-MBNL1 complex and improve DM1-associated molecular defects *in vitro* and in some cases also *in vivo*. Several approaches were successful in identifying small molecules, such as screening of known nucleic acid binders (21), rational design of small molecules based on the structure of $(CUG)_n$ RNA (22), rational design of oligomers of $(CUG)_n$ RNA binders by modular assembly (23, 24), combinatorial chemistry (25, 26), and high-throughput screening (27, 28).

* This work was funded by the Neuromuscular Research Association Basel, Swiss National Science Foundation, and by Myosuisse. The authors declare that they have no conflicts of interest with the contents of this article.
[1] Supported by Swiss Federal Commission for Scholarship for Foreign Students (FCS) and South African National Research Foundation fellowships.
[2] To whom correspondence may be addressed: Neuromuscular Research Group, Depts. of Neurology and Biomedicine, University Hospital Basel, Klingelbergstr. 50, 4056 Basel, Switzerland. Tel.: 41-61-2671635; E-mail: j.kinter@unibas.ch.
[3] To whom correspondence may be addressed: Neuromuscular Research Group, Depts. of Neurology and Biomedicine, University Hospital Basel, Klingelbergstr. 50, 4056 Basel, Switzerland. Tel.: 41-61-2652525; E-mail: michael.sinnreich@unibas.ch.
[4] The abbreviations used are: DM1, myotonic dystrophy type 1; DMPK, dystrophia myotonica protein kinase; HSA^{LR}, human skeletal α-actin long repeat; qPCR, quantitative PCR; DHB, dihydroberberine; GM, growth medium.

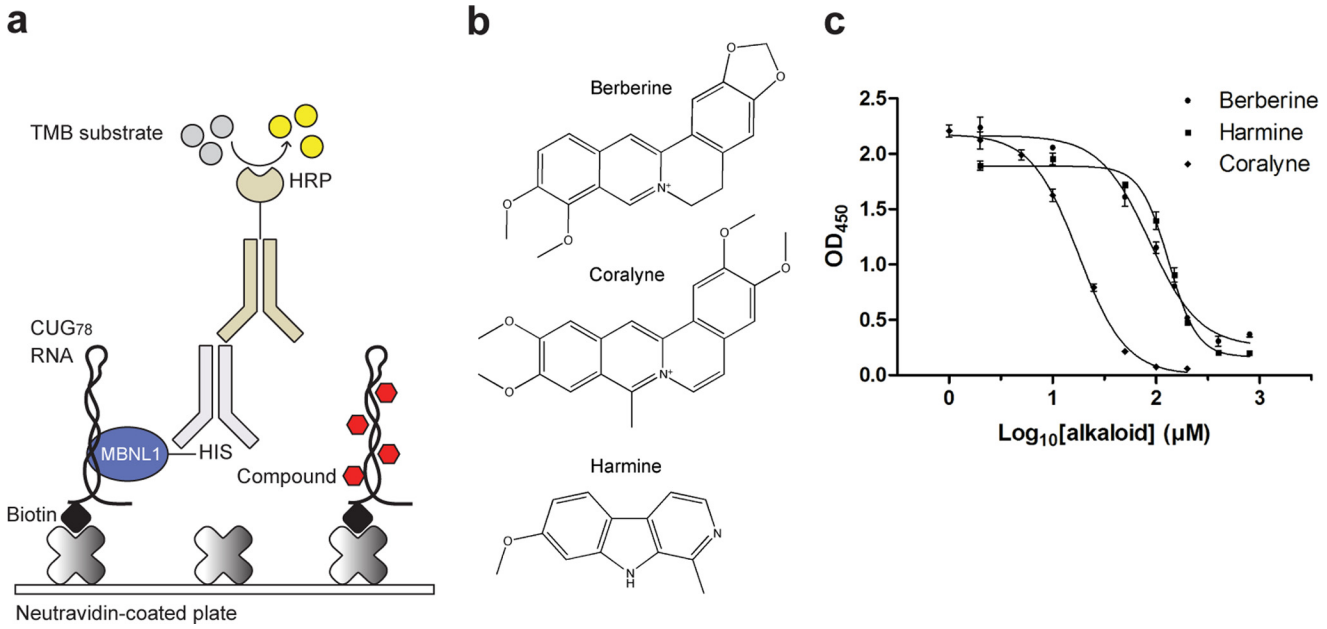

FIGURE 1. **Screening for small molecules of natural origin that disrupt the CUG_{78}-MBNL1 complex *in vitro*.** *a*, the CUG_{78}-MBNL1 inhibition assay detects the amount of MBNL1 bound to CUG_{78}-RNA. *b*, structure of the identified alkaloids berberine, coralyne, and harmine. *c*, CUG_{78}-MBNL1 complex inhibition curves. *OD*, optical density; *TMB*, 3,3′,5,5′-tetramethylbenzidine.

Most of the described $(CUG)_n$ RNA-targeting molecules are synthetic. Only a few small molecules of natural origin have been described, such as neomycin B (21) and lomofungin (27). To our knowledge, our study is the first to focus on small molecules of natural origin and represents the first screening of natural extracts in DM1 drug discovery. As RNA is still a relatively unexploited drug target, natural products present a rich source of new and diverse RNA binders (29). Interestingly, many known RNA-binding drugs are of natural origin, such as antibiotics that target the bacterial ribosomal RNA (30). Hence, it is of interest to investigate natural products in drug discovery for RNA-mediated diseases such as DM1.

We describe here the screening of isolated natural compounds and extracts from plants and fungal strains in a novel CUG_{78}-MBNL1 complex inhibition assay. We identified several alkaloids as CUG_{78}-MBNL1 complex inhibitors. Testing their bioactivity in a human myoblast model of DM1 (31) and in the human skeletal α-actin long repeat (HSA^{LR}) mouse model of DM1 (4) showed that the alkaloids ameliorate certain aspects of the DM1 pathology.

Results

CUG_{78}-MBNL1 Complex Inhibitors of Natural Origin—A collection of 70 isolated natural compounds and a library containing 2128 extracts from plants and fungi were screened with a novel *in vitro* CUG_{78}-MBNL1 complex inhibition assay (Fig. 1*a*). Biotinylated CUG_{78} RNA was immobilized on NeutrAvidin-coated plates that were then co-incubated with MBNL1-HIS and compounds or extracts. The plates were washed to remove unbound components, and MBNL1-HIS in complex with immobilized CUG_{78} RNA was detected via an anti-HIS and a secondary HRP-conjugated antibody. The library of isolated natural compounds was screened at 100 μM concentration and led to the identification of the isoquinoline alkaloid berberine (Fig. 1*b*) as a complex formation inhibitor with an IC_{50} of 86.3 ± 5.8 μM (Fig. 1*c*). Another alkaloid, isaindigotone, showed weak inhibitory activity at 100 μM concentration. From the extract library we identified 21 extracts that inhibited CUG_{78}-MBNL1 complex formation by 40–82% at a concentration of 100 μg/ml compared with solvent-only controls. Seven extracts were chosen for fractionation. To identify the active principles in these extracts, we used an approach referred to as HPLC-based activity profiling. It combines the separation of complex mixtures with spectroscopic data recorded online and with biological information obtained in parallel from time-based microfractionation and a subsequent bioassay (32). In addition, offline microprobe NMR analysis was used to fully establish the structure of active compounds. The alkaloid harmine (Fig. 1*b*) was identified as an active constituent in a methanolic extract from the roots of *Peganum harmala* (Nitrariaceae) (Fig. 2*a*). Besides, two closely related diterpenequinones, methylenetanshinquinone and 1,2-dihydrotanshinquinone, were detected in the active fractions of an ethyl acetate extract from roots of *Salvia miltiorrhiza* (Lamiaceae) (Fig. 2*b*). A commercial sample of harmine had an IC_{50} of 132.4 ± 9.3 μM (Fig. 1*c*), whereas the two diterpenequinones, also commercially obtained, showed weak inhibitory activity at 100 μM concentration. The inhibitory activity of the remaining extracts could be assigned to tannins. These extracts lost their complex inhibitory effect after filtration through a polyamide cartridge to remove polyphenolic tannins.

The alkaloids berberine and harmine were chosen for further study. We tested a small set of structural analogues of berberine and identified coralyne (Fig. 1*b*), a planar berberine derivative, as a stronger CUG_{78}-MBNL1 complex inhibitor with an IC_{50} of 17.8 ± 0.2 μM (Fig. 1, *b* and *c*). As reference compounds, Hoechst 33258 and neomycin B, two known nucleic acid bind-

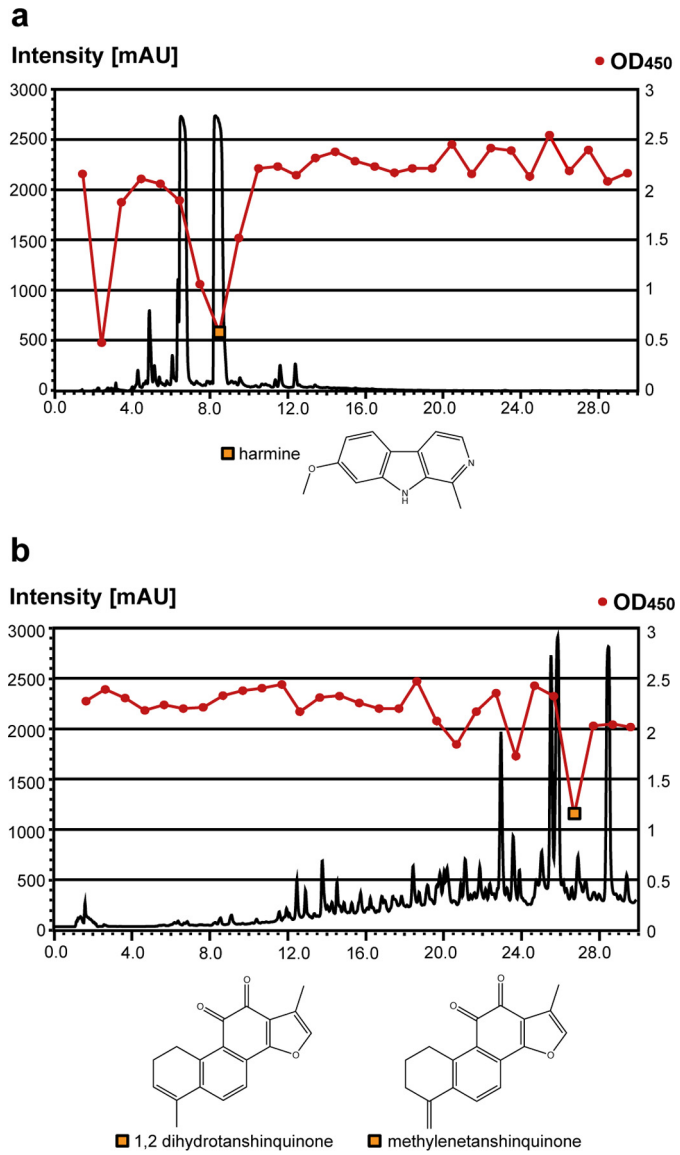

FIGURE 2. *a*, HPLC-based activity profiling of the *P. harmala* methanol extract. Shown on the *y* axis are the online HPLC-UV trace at 254 nm (*black*) and the A_{450} signal from the CUG_{78}-MBNL1 inhibition assay (*red*). The *x* axis shows the time in minutes. 29 fractions were collected, 1 min each. The inhibitory activity of the fraction at minutes 8–9 was assigned to the alkaloid harmine. Based on online MS and UV spectroscopic data, the other major peak eluting at 6.6 min was assigned to harmol. The activity in the early-eluting fraction, 2–3 min, did not correspond to any UV peak and was not further investigated. *OD*, optical density; *mAU*, milli absorbance units. *b*, HPLC-based activity profiling of the ethyl acetate extract of *S. miltiorrhiza*. The inhibitory activity of the fraction at minutes 26–27 was assigned to two diterpenequinone isomers, 1,2-dihydrotanshinquinone and methylenetanshinquinone.

ers, were tested and had IC_{50} values of 195.5 ± 3.0 μM and 5.3 ± 0.6 μM, respectively.

Identified Alkaloids Improve Splicing in Human DM1 Myoblasts—The alkaloids identified in our *in vitro* screening assay were tested for their ability to ameliorate splicing in a human DM1 myoblast cell line containing a CTG_{1300} repeat in the 3′ UTR of the DMPK gene (31). The WT control cell line contained a normal repeat length in the same locus. Differentiated DM1 myoblasts were treated with the identified alkaloids, and alternative splicing was analyzed by a quantitative PCR (qPCR) method using two primer pairs. This method allowed real-time quantitation of the inclusion/exclusion of an investigated alternatively spliced exon.

Berberine improved the splicing of the *TNNT2* pre-mRNA exon 5. In 80 μM berberine-treated DM1 myoblasts, the splicing was close to that of the WT control myoblasts. *TNNT2* pre-mRNA splicing was rescued by 62.1% ± 3.2% ($p = 0.001$, Student's *t* test, 20 μM), 75.1% ± 2.8% ($p = 0.0006$, 40 μM), and 86.2% ± 0.8% ($p = 0.0003$, 80 μM) through berberine treatment (Fig. 3*a*). However, berberine treatment had a negative effect on *INSR* pre-mRNA exon 11 splicing (Fig. 3*a*) in DM1 myoblasts. In contrast to berberine, harmine improved both the splicing of the *TNNT2* pre-mRNA exon 5 by 53.3% ± 3.5% ($p = 0.003$, 20 μM), 76.8% ± 1.6% ($p = 0.0005$, 40 μM), and 66.1% ± 1.2% ($p = 0.0009$, 80 μM), and, furthermore, the splicing of the *INSR* pre-mRNA exon 11 by 6.3% ± 0.3% ($p = 0.003$, 40 μM) and 55.4% ± 3.3% ($p = 0.0003$, 80 μM) (Fig. 3, *a* and *b*). The alternative splicing results obtained with the qPCR method for berberine and harmine were confirmed with classical RT-PCR and visualization of two alternatively spliced isoforms of the *INSR* and *TNNT2* pre-mRNA on 3% agarose gels (Fig. 3, *c* and *d*). The synthetic berberine derivative coralyne and the two diterpenequinones, identified together with harmine during the extract screening, showed no effect on splicing in the DM1 cell model.

To investigate the selectivity of berberine and harmine, we tested their effect on alternative splicing of two genes known to be alternatively spliced but independent of MBNL1, *i.e. ATE1* and *FHL1* (Fig. 3, *e* and *f*) (33). We analyzed exon 7 inclusion in the *ATE1* pre-mRNA, which was close to 33% for the WT cell line and close to 40% in the DM1 cell line. Exon 5 inclusion in the *FHL1* pre-mRNA was close to 0.1–0.2% for both the WT and the DM1 cell line. The levels of alternative exon inclusion in berberine- and harmine-treated (both at 20 μM and 80 μM) myoblasts were in the range of the levels of vehicle-treated WT and DM1 control myoblasts. The qPCR analysis of the harmine effect on *TNNT2* pre-mRNA alternative splicing in WT myoblasts showed an enhancement of MBNL1-dependent splicing analogous to harmine-treated DM1 myoblasts. This effect, however, was only observed with the qPCR method and not visible by the classical RT-PCR method (Fig. 3, *b* and *d*).

The cellular toxicity of berberine and harmine was determined in a viability assay with C2C12 mouse myoblasts. Concentrations (toxicity IC_{50}) were determined at which half of the myoblasts remained viable after 2 days of compound incubation. Berberine yielded a toxicity IC_{50} of 212.1 ± 18.3 μM and harmine one of 123.3 ± 4.6 μM. Mitomycin C was measured as reference compound with a toxicity IC_{50} of 20.4 ± 1.6 μM. Although the IC_{50} and toxicity IC_{50} values were relatively close for both alkaloids, both compounds showed an effect on alternative splicing in the myoblast model at concentrations significantly lower than the IC_{50} and toxicity IC_{50} values, *e.g.* at 20 μM (Fig. 3).

Harmine Reduces Focus Formation in Human DM1 Myoblasts—To examine whether the alkaloids berberine and harmine reduce the sequestration of MBNL1 by $(CUG)_n$ RNA, focus formation was investigated in the two human myoblast cell lines. Immunofluorescence staining in both the WT (nor-

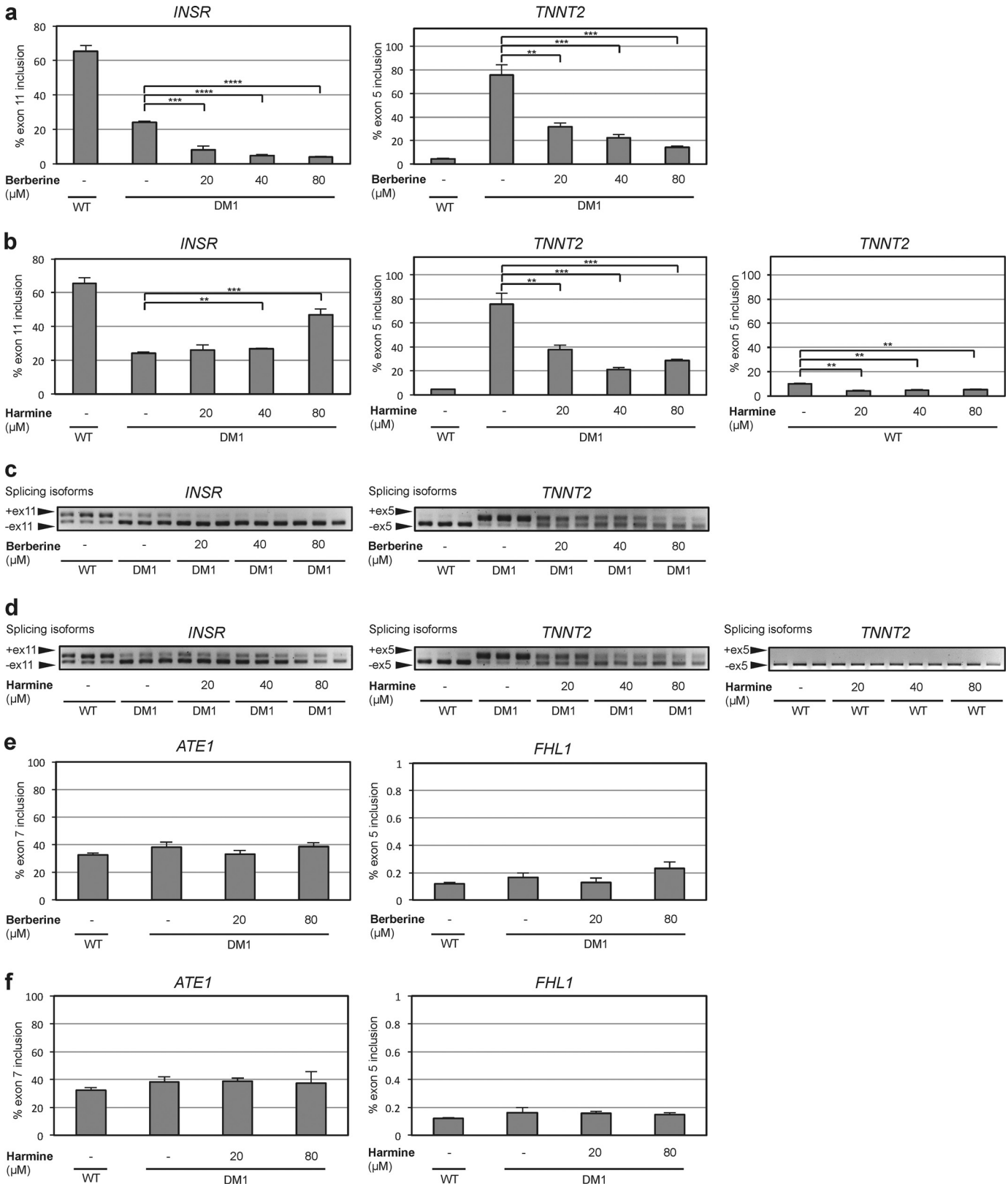

FIGURE 3. **Representative qPCR splicing data for WT and DM1 control myoblasts and treated human myoblasts.** The percentage of alternative exon inclusion is shown. *a*, berberine improves the splicing of the *TNNT2* pre-mRNA but has a detrimental effect on the *INSR* pre-mRNA splicing. *b*, harmine improves the splicing of both the *TNNT2* and of the *INSR* pre-mRNA. Harmine also promotes MBNL1-dependent splicing in treated WT myoblasts, as shown for the *TNNT2* pre-mRNA. *c* and *d*, RT-PCR analysis of *INSR* and *TNNT2* pre-mRNA alternative splicing. Visualized on 3% agarose are two alternative splicing isoforms for both pre-mRNAs in untreated WT and DM1 control myoblasts and DM1 myoblasts treated with (*c*) berberine and (*d*) harmine. The harmine effect on MBNL1-dependent splicing in treated WT myoblasts was not visible with this method, as shown for the *TNNT2* pre-mRNA. *e* and *f*, berberine and harmine do not affect alternative splicing of MBNL1-independently regulated *ATE1* and *FHL1* pre-mRNAs in treated DM1 myoblasts compared with untreated WT and DM1 control myoblasts. **, $p \leq 0.01$; ***, $p \leq 0.001$; ****, $p \leq 0.0001$.

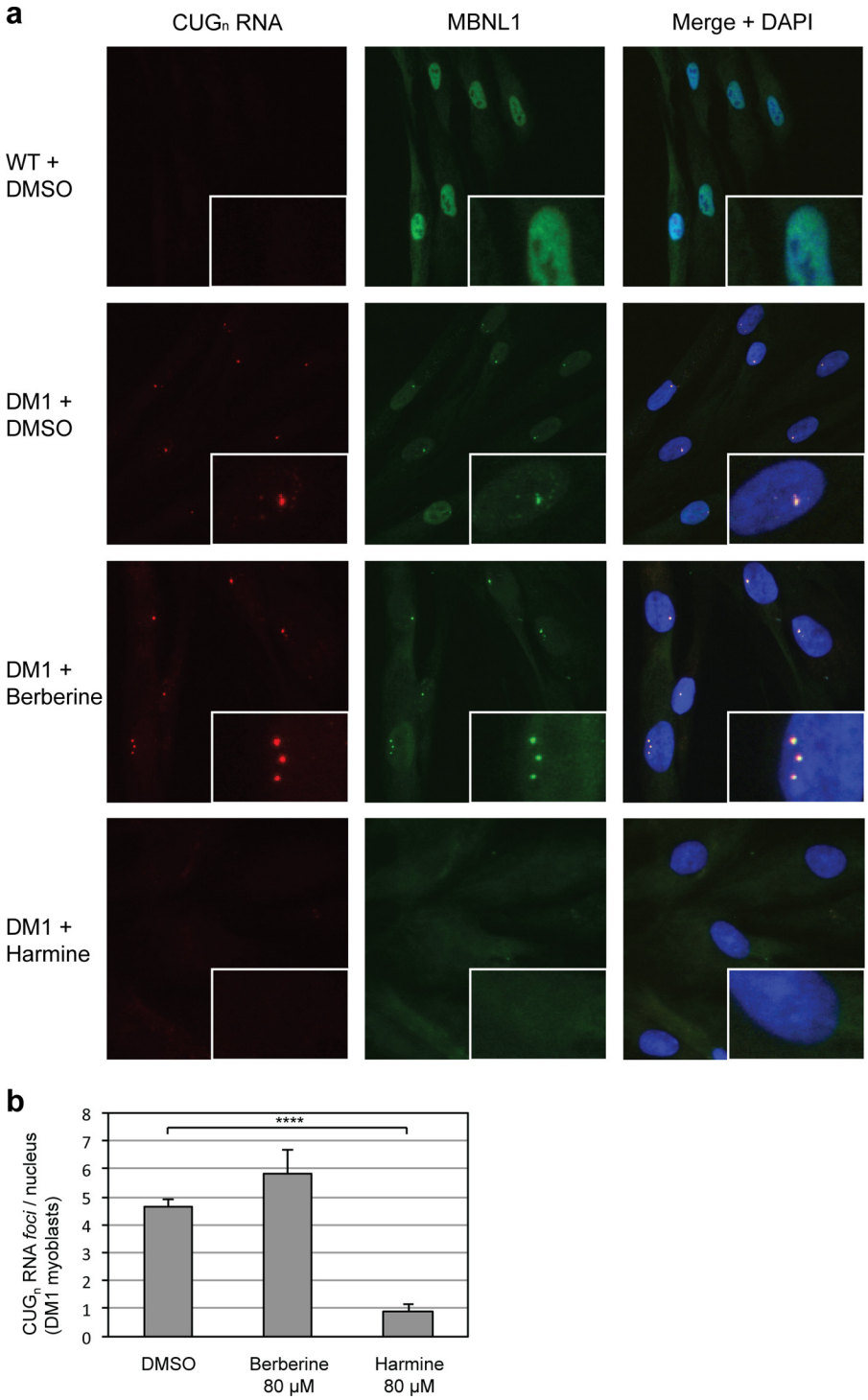

FIGURE 4. **Analysis of foci with FISH and immunofluorescence.** *a*, harmine reduces the amount of foci at 80 μM concentration, whereas berberine does not reduce foci. For each condition, $(CUG)_n$ RNA staining (*red*), MBNL1 staining (*green*), and a merge of both with nuclear DAPI staining (*blue*) is shown. Vehicle-treated control WT and DM1 myoblasts and compound-treated (80 μM) myoblasts are shown. *b*, quantification of the number of foci in human DM1 myoblasts either treated with vehicle or alkaloids at 80 μM. ****, $p \leq 0.0001$.

mal CUG repeat length) and the DM1 (CUG_{1300}) cell line showed that MBNL1 was mainly localized to the nuclei. In the DM1 cells, punctate staining of MBNL1 within the nucleus could be co-localized in foci with $(CUG)_n$ RNA, visualized by fluorescence *in situ* hybridization. Treatment with 80 μM harmine significantly reduced ($p = 0.00005$, Student's *t* test) the quantity of foci in DM1 myoblasts (Fig. 4*a*) to 0.9 $\pm$ 0.2 foci per nucleus compared with DMSO-treated DM1 myoblasts with 4.7 $\pm$ 0.3 foci per nucleus (Fig. 4, *a* and *b*). Harmine-treated myoblasts lost their punctate nuclear MBNL1 staining, indicative of MBNL1 release from the toxic $(CUG)_n$ RNA, although the nuclear MBNL1 staining pattern of WT myoblasts was not regained. We analyzed by Western immunoblotting whether treatment with harmine reduced the levels

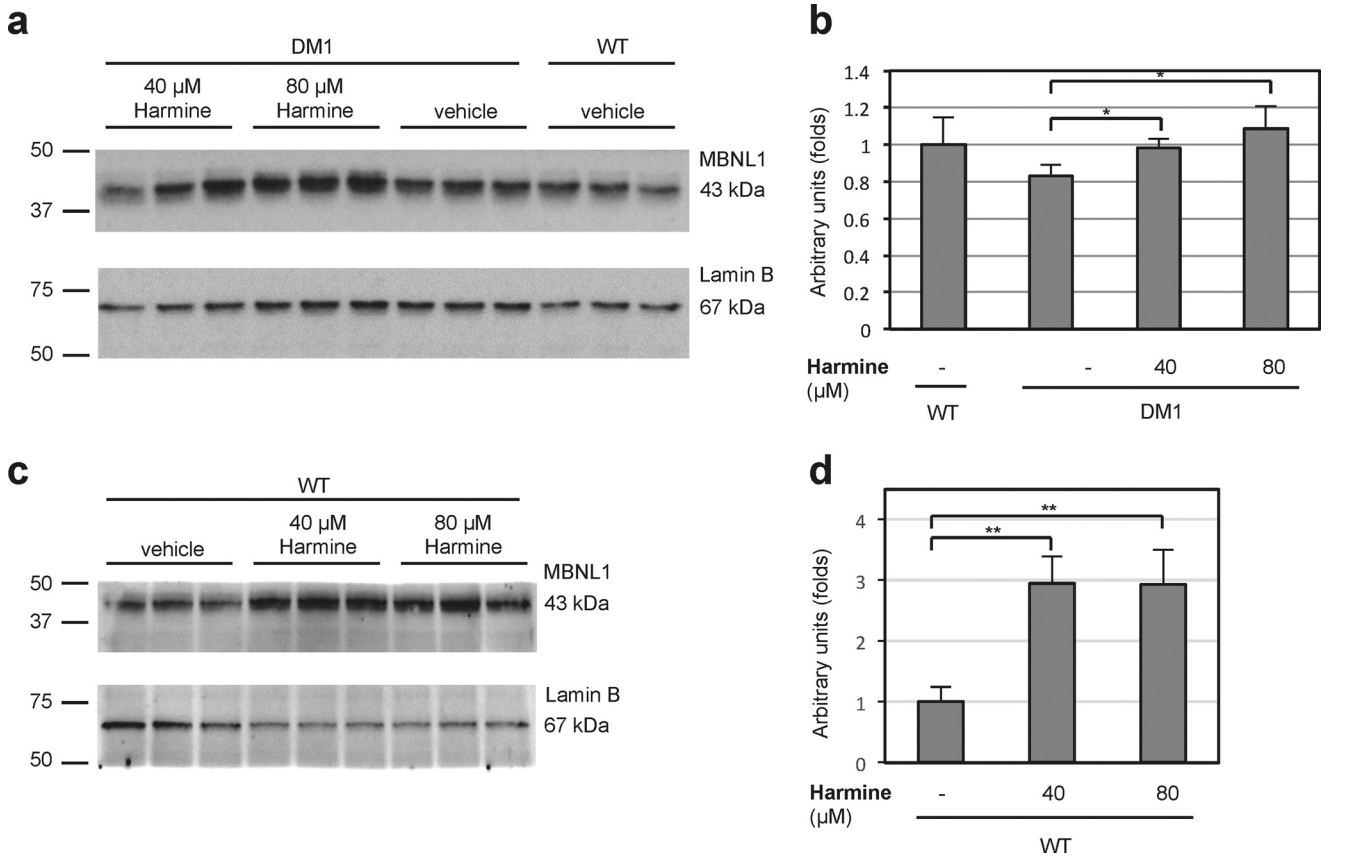

FIGURE 5. *a*, Western blot showing MBNL1 protein levels of DM1 myoblasts treated with 40 and 80 μM harmine, of vehicle-treated DM1 myoblasts, and of vehicle-treated WT myoblasts (*left* to *right*). *b*, quantification of MBNL1 band intensities normalized to lamin B. The means of three replicates for each condition, including the standard deviation, are shown. *c*, Western blot showing MBNL1 protein levels of WT myoblasts treated with vehicle or 40 and 80 μM harmine (*left* to *right*). *d*, quantification of MBNL1 band intensities normalized to lamin B. The means of three replicates for each condition, including the standard deviation, are shown. *, $p \leq 0.05$; **, $p \leq 0.01$.

of MBNL1 in cell lysates of treated DM1 myoblasts to account for the reduced nuclear staining and found that harmine in fact increased the total levels of MBNL1 in treated DM1 myoblasts compared with vehicle-treated control DM1 myoblasts (Fig. 5, *a* and *b*). An increase in MBNL1 levels was also observed in harmine-treated WT myoblasts (Fig. 5, *c* and *d*). 80 μM berberine treatment of DM1 myoblasts led to a statistically insignificant increase ($p = 0.099$) in the number of foci to 5.8 ± 0.9 foci per nucleus in the DM1 myoblast cell line (Fig. 4, *a* and *b*).

Identified Alkaloids Ameliorate Splicing of CLCN1 Pre-mRNA in HSA^{LR} Mice—Next, we treated HSA^{LR} mice, a DM1 model containing a CTG_{250} repeat expressed under a human skeletal actin promoter (4), with the identified alkaloids. The compounds were tested for their ability to restore splicing of CLCN1 (12, 13) and SERCA1 (15) pre-mRNA in quadriceps muscle. MBNL1 promotes the exclusion of the alternatively spliced exon 7a of the CLCN1 pre-mRNA and promotes the inclusion of exon 22 of the SERCA1 pre-mRNA (12, 13, 15). Vehicle-treated WT mice at the age of 10–12 weeks showed a CLCN1 pre-mRNA exon 7a inclusion of 5.0% ± 0.5%, whereas, in vehicle-treated HSA^{LR} mice, the inclusion level was elevated to 40.9% ± 2.5%. The level of SERCA1 pre-mRNA exon 22 inclusion in WT mice was at 83.9% ± 2.9%. In HSA^{LR} mice, exon 22 inclusion was decreased to 24.8% ± 2.7%. We first tested berberine, which, at a dose of 20 mg/kg, led to reduced activity and decreased body temperature, which urged us to lower the dose. Treatment with 5 mg/kg and 10 mg/kg of berberine did not result in any significant splicing improvement. We then tested two close derivatives of berberine, dihydroberberine (DHB) and palmatine, with higher reported LD_{50} values. DHB improved the splicing of the CLCN1 pre-mRNA at a dose of 10 mg/kg by 32.5% ± 2.9% ($p = 0.0008$, Student's *t* test), whereas 5 mg/kg showed no statistically significant effect (Fig. 6*a*). The CLCN1 splicing improvement with 10 mg/kg DHB was confirmed by classical RT-PCR and analysis of splicing isoforms on a 3% agarose gel (Fig. 6*d*). Palmatine treatment improved CLCN1 pre-mRNA splicing at a dose of 40 mg/kg by 34.8% ± 2.1% ($p = 0.0009$) and at a dose of 25 mg/kg by 25.3% ± 0.7% ($p = 0.0017$), whereas 10 mg/kg did not show a significant effect (Fig. 6*b*). Harmine treatment at a dose of 40 mg/kg decreased CLCN1 pre-mRNA exon 7a inclusion by 31.2% ± 1.7% ($p = 0.0003$) and did not significantly improve splicing at a dose of 20 mg/kg (Fig. 6*c*). Side effects observed during harmine treatment were transient tremors. DHB, palmatine, and harmine had no significant effect on SERCA1 pre-mRNA splicing (Fig. 6).

CLCN1 Protein Levels in Quadriceps Muscle of WT, HSA^{LR}, and Treated HSA^{LR} Mice—We examined by Western immunoblotting analysis whether the high-dose alkaloid treatments,

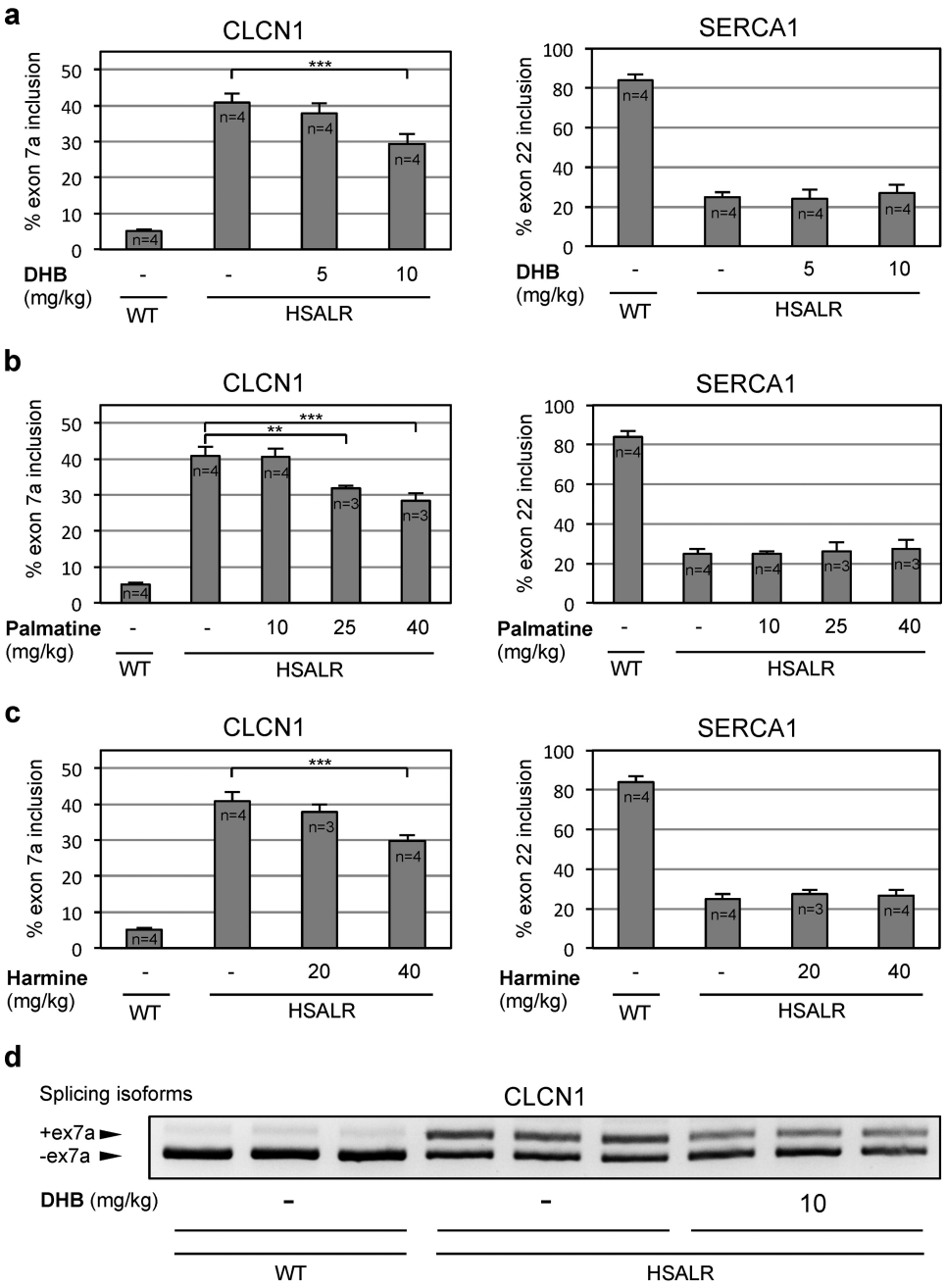

FIGURE 6. **Representative qPCR splicing data for vehicle-treated WT and HSA^{LR} mice and compound-treated HSA^{LR} mice (quadriceps muscle).** Shown is the percentage of exon 7a (*CLCN1*) and exon 22 (*SERCA1*) pre-mRNA inclusion. The alkaloids improve the splicing of CLCN1, whereas the splicing of SERCA1 is unchanged. *a*, DHB treatment. *b*, palmatine treatment. *c*, harmine treatment. *d*, alternative splicing of the CLCN1 pre-mRNA analyzed by RT-PCR and visualized on 3% agarose gel. Shown are two alternative splicing isoforms in vehicle-treated control mice and DHB-treated HSA^{LR} mice. **, $p \leq 0.01$; ***, $p \leq 0.001$.

which had ameliorated CLCN1 pre-mRNA splicing, also increased the protein levels of the full-length CLCN1 channel *in vivo*. CLCN1 protein levels in quadriceps muscle of four vehicle-treated HSA^{LR} mice were decreased by 29.1% ± 12.4% ($p = 0.023$, Student's *t* test, $n = 4$, three immunoblots) compared with four vehicle-treated WT mice (Fig. 7). Treatment of HSA^{LR} mice with 10 mg/kg DHB raised CLCN1 protein levels by 27.1% ± 16.1% ($p = 0.095$, $n = 4$) compared with levels of vehicle-treated HSA^{LR} mice (Fig. 7). Although the CLCN1 protein levels of DHB-treated HSA^{LR} mice were close to WT levels, the effect did not reach statistical significance. Both palmatine and harmine high-dose treatments of 40 mg/kg did not increase the CLCN1 protein levels in HSA^{LR} mice (Fig. 7).

Analysis of Internalized Nuclei in Gastrocnemius Muscle Sections of Vehicle-treated WT, HSA^{LR}, and Harmine-treated HSA^{LR} Mice—Despite the very short treatment duration of only 14–16 h (two injections at a 12-h interval), we wished to examine whether the most promising small molecule, harmine, also improved the histology in gastrocnemius muscle of harmine-treated mice (Fig. 8). Different histological parameters were analyzed, most importantly the percentage of fibers with inter-

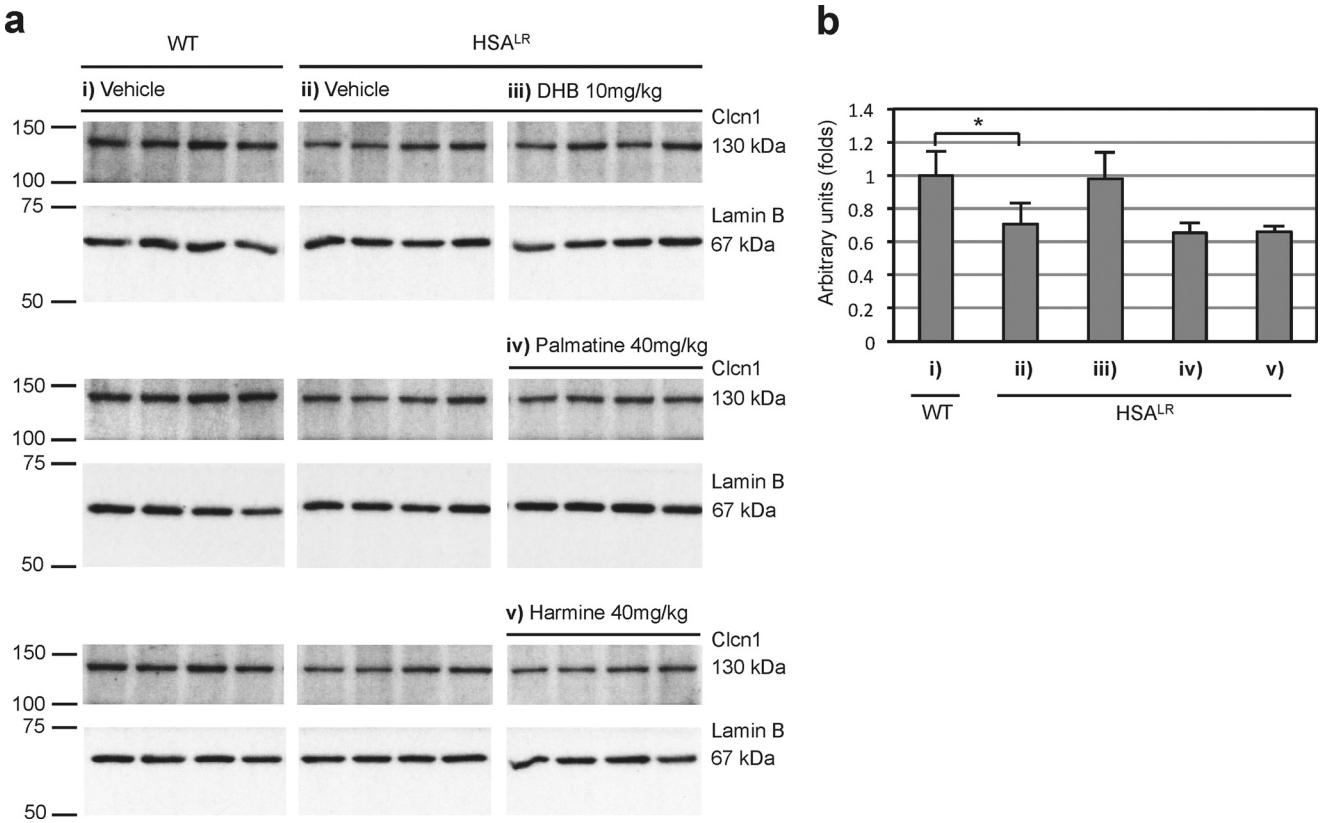

FIGURE 7. *a*, Western blot showing CLCN1 protein levels of (*i*) vehicle-treated WT mice, (*ii*) vehicle-treated HSA^{LR} mice, and (*iii–v*) compound-treated HSA^{LR} mice. *b*, quantification of CLCN1 band intensities normalized to lamin B. The means of four replicates for each condition, including the standard deviation, are shown. *, $p \leq 0.05$.

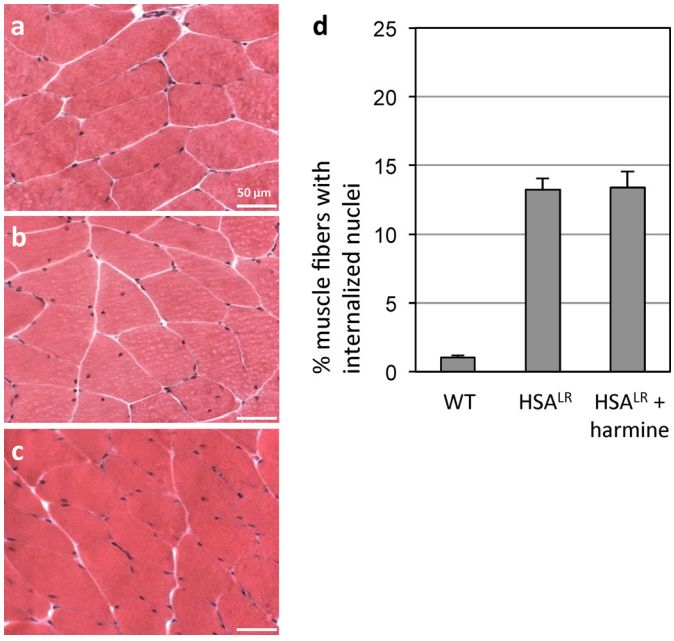

FIGURE 8. Shown is the analysis of internalized nuclei by H&E staining of 8-μm mouse gastrocnemius muscle cross-sections of 10-week-old (*a*) vehicle-treated WT mice, (*b*) vehicle-treated HSA^{LR} mice, and (*c*) HSA^{LR} mice after treatment by two injections of 40 mg/kg harmine at a 12-h interval. *d*, quantitative analysis of the percentage of muscle fibers with internalized nuclei.

nalized nuclei, where no difference was detected between vehicle-treated and harmine-treated HSA^{LR} mice after this short treatment duration.

Discussion

We report the discovery of several plant-derived alkaloids as novel bioactive small molecules with therapeutic potential for DM1. Through inhibition of the $(CUG)_n$-MBNL1 complex, the alkaloids ameliorate certain aspects of the DM1 pathology. Our screening of natural products identified the alkaloids berberine and harmine, which were chosen for further study. Interestingly, both have been described previously to bind to specific RNA structures, such as double-stranded RNA, tRNA, and poly(A) RNA (34–37). The berberine derivative coralyne has been described as a complete intercalator for double-stranded RNA and berberine as a partial intercalator (36). We therefore hypothesize that the binding of these three aromatic alkaloids to the double-stranded $(CUG)_n$ RNA may involve intercalation because of planarity. Aromatic alkaloids such as berberine, coralyne, and harmine might be of particular interest for RNA drug discovery, as they can interact with RNA via stacking (intercalation), hydrogen bonding, or electrostatic interaction (38). To our knowledge, in the context of DM1, no alkaloids have been described so far. An *in vitro* screening study by Chen *et al.* (28) yielded six hits of which four were alkaloids or alkaloid derivatives of the opioid- and ergot alkaloid-type, but none of these alkaloids could be confirmed in a secondary assay .

Berberine and harmine showed partially positive effects on splicing and focus formation in a human DM1 cell line. Harmine showed positive effects in most of the studied models. It inhibited CUG_{78}-MBNL1 complex formation *in vitro* and ameliorated the pre-mRNA splicing of both the *INSR* exon 11

and *TNNT2* exon 5 in the human DM1 myoblast cell line, where it also reduced the formation of foci without decreasing MBNL1 protein levels. Interestingly, harmine enhanced MBNL1-dependent alternative splicing to a comparable relative extent in both DM1 and WT myoblasts, indicating that harmine does not act primarily via $(CUG)_n$-MBNL1 complex disruption but, rather, via another mechanism leading to increased MBNL1 protein levels. We could not detect a significant difference of *TNNT2* pre-mRNA splicing in myotubes upon harmine treatment, although a trend toward MBNL1-mediated alternative splicing was visible (data not shown).

Harmine also improved the splicing of CLCN1 pre-mRNA in the HSA^{LR} DM1 mouse model at a high dose of 40 mg/kg. Even though 40 mg/kg harmine treatment ameliorated CLCN1 splicing in HSA^{LR} mice, it did not affect the histology of these mice. This was, however, expected because of the short treatment duration of only 14–16 h. Berberine did not perform as well as harmine in the studied models. Although it was a stronger CUG_{78}-MBNL1 complex inhibitor than harmine, it only improved the splicing of the *TNNT2* pre-mRNA in the DM1 myoblast cell line, whereas the splicing of the *INSR* pre-mRNA was worsened in treated DM1 myoblasts. This undesirable splicing effect of berberine might be due to insufficient selectivity of berberine for the $(CUG)_n$ RNA over the MBNL1 binding motifs in pre-mRNAs and, therefore, interference with MBNL1-mediated splicing. MBNL1-targeted pre-mRNAs as the toxic DMPK-$(CUG)_n$ transcripts have similar MBNL1 binding motifs (39). Interestingly, the berberine derivative coralyne was an even stronger CUG_{78}-MBNL1 complex inhibitor than berberine but showed no effect on splicing in the DM1 cell model. Coralyne is a nonspecific intercalator for double-stranded RNA (36). Its insufficient selectivity for the $(CUG)_n$ RNA over other double-stranded RNAs might be the reason for lacking specific bioactivity. Like coralyne, the two identified diterpenequinones, methylenetanshinquinone and 1,2-dihydrotanshinquinone, lacked bioactivity. As the two planar diterpenequinones were poorly water-soluble, they precipitated at higher concentrations in the screening assay and precipitated from solution in cell culture at concentrations of 20 and 40 μM. Among all identified compounds during our screening of natural products, planarity and aromaticity turned out to be common features, and the partly double-stranded $(CUG)_n$ RNA target selects for planar molecules with intercalating properties.

The evaluation of the alkaloids berberine, dihydroberberine, palmatine, and harmine in the HSA^{LR} mouse model showed promising results. Most interestingly, two alkaloids of the berberine type, DHB and palmatine, and the alkaloid harmine significantly improved the splicing of the CLCN1 pre-mRNA in this mouse model. The alkaloid DHB was the most active alkaloid, as it improved CLCN1 exon 7a splicing at a dose of 10 mg/kg. However, these alkaloids are not suited for therapeutic application themselves. Their relatively low potency and toxicity are issues that require medicinal chemistry optimization. Berberine has been described as an inhibitor of complex I in the mitochondrial respiratory chain (40). Hence, decreased metabolic activity might account for the side effects we observed upon treatment with berberine and its derivatives at high doses, *i.e.* reduced activity and decreased body temperature. The effect of berberine on thermoregulation in mice has been described previously by Jiang *et al.* (41). In harmine-treated mice we observed tremors after administration. Harmine has been described as a tremorogenic substance (42). Berberine, its derivatives DHB and palmatine, as well as harmine exert CNS effects given that they are monoamine oxidase inhibitors (43, 44). These side effects need to be addressed by medicinal chemistry modifications. However, the fact that these alkaloids penetrate the blood-brain barrier stirs hope for a future small-molecule therapy that also ameliorates the DM1-associated CNS pathology. Moreover, the identified molecules help to further understand the characteristics of small molecules that interact with toxic $(CUG)_n$ RNA and provide new chemical scaffolds for medicinal chemistry studies. Particularly harmine, with its low molecular weight of 212.25 Da, offers an appealing starting point for chemical modifications. Harmine furthermore represents an interesting molecule, as its biological effect is likely not mediated only by liberation of MBNL1 from toxic $(CUG)_n$ RNA, which was initially assumed based on results from the *in vitro* CUG_{78}-MBNL1 inhibition screening assay, but mainly via another, yet unidentified mechanism leading to an increase in MBNL1 protein levels in treated myoblasts. This effect will be investigated in more detail in follow-up studies. Our study thus contributes to further progress in small-molecule drug discovery for this disabling neuromuscular disease.

Experimental Procedures

Statistical Analysis—Unless otherwise stated, results are expressed as mean ± S.D. of $n \geq 3$ independent experiments. Comparisons between two conditions were performed using Student's *t* test with a 0.05 confidence level accepted for statistical significance (*, $p \leq 0.05$; **, $p \leq 0.01$; ***, $p \leq 0.001$; ****, $p \leq 0.0001$).

Compounds and Extracts—The compounds and extracts screened in this study were part of natural product libraries established at the Division of Pharmaceutical Biology of the University of Basel. One library contained 70 pure natural compounds as 10 mM solutions in DMSO, and a second library consisted of 2128 extracts from plants and fungi archived as 10 mg/ml solutions in DMSO (32). Harmine hydrochloride was purchased from TCI Europe (H0002). Berberine chloride (B3251), palmatine chloride hydrate (361615), and coralyne sulfoacetate (S424536) were obtained from Sigma-Aldrich. Dihydroberberine (80429) was purchased from PhytoLab GmbH. Methylenetanshinquinone (QP-393) and 1,2-dihydrotanshinquinone (QP-1166) were obtained from Quality Phytochemicals LLC (East Brunswick, NJ). The reference substances neomycin B (N1876), Hoechst 33258 (B2883), and mitomycin C (M4287) were ordered from Sigma-Aldrich.

MBNL1 Preparation—MBNL1 cDNA (an isoform with amino acids 1–382) was kindly provided by Maurice Swanson (9) (University of Florida). The pGEX-6P-MBNL1-N-His (amino acids 1–253) construct used in this study was cloned according to Yuan *et al.* (9), and protein expression and purification were performed similar to the procedure published by Yuan *et al.* (9). MBNL1-HIS was stored in a buffer containing 10 mM Tris (pH 7.4), 50 mM NaCl, and 1 mM DTT. Protein concentration was determined with a NanoDrop spectrophotom-

eter and a BCA assay (Sigma). The purity of MBNL1-HIS was evaluated by means of SDS-PAGE followed by Coomassie staining. MBNL1-HIS aliquots were snap-frozen in liquid nitrogen and stored at −70 °C.

CUG_{78} RNA Preparation—Genomic DNA was isolated from a patient blood sample (with informed consent) with the Puregene Blood Core Kit B (Qiagen) according to the protocol of the manufacturer. A CTG_{78}-containing genomic DMPK fragment was PCR-amplified with HOT Start DNA polymerase (Solis BioDyne) and the following primers: DMPK forward, 5′CAGCTCCAGTCCTGTGATCC3′; DMPK reverse, 5′CTGGCCGAAAGAAAGAAATG3′. The amplicon was agarose gel-purified with the QIAquick gel extraction kit (Qiagen). The purified DNA fragment was cloned by TA cloning with the pCR II-TOPO plasmid vector in Dh5α bacterial cells. The plasmid was purified with the QIAprep spin miniprep kit (Qiagen) and used as a template for PCR amplification with the following primers: T7 CUG forward, 5′TAATACGACTCACTATAGGCAGCTCCAGTCCTGTGATCC3′; and T7 CUG reverse, 5′TAATACGACTCACTATAGGCTGGCCGAAAGAAAGAAATG3′. The amplified DNA was purified with the QIAquick PCR purification kit (Qiagen). 200 ng of DNA was used as a template for *in vitro* RNA transcription with the MEGAscript T7 transcription kit (Ambion). CUG_{78} RNA was biotin-labeled by addition of 1.875 mM biotin-14-CTP (37.5 nmol). RNA quality and purity was tested by visualization of RNA on 8 M urea/Tris borate-EDTA 5% polyacrylamide gels.

CUG_{78}-MBNL1 Inhibition Assay—Wash steps were performed at room temperature with 150 μl of wash buffer/well (25 mM Tris (pH 7.4), 80 mM NaCl, 1 mM $MgCl_2$, 0.5 mM DTT, 0.05% Tween 20, 1.5 mg/ml BSA, and diethylpyrocarbonate-treated water) and incubation steps with 50 μl of incubation buffer/well (wash buffer + 25 units/ml RNasin (Promega)) at 30 °C on a BIOSAN plate shaker at 300 rpm. Reacti-Bind NeutrAvidin-coated 96-well plates (Pierce) were prewashed once. Wash buffer was removed, and incubation buffer containing 25 ng of biotinylated CUG_{78} RNA was added/well. After incubation for 1 h, the plates were washed twice. Wash buffer was removed, and 45 μl of incubation buffer containing 300 ng of MBNL1-HIS was added, followed by addition of 5 μl of 10× concentrated compound or 5 μl of DMSO/water for controls. After washing wells twice, mouse anti-HIS antibody (1:2000, GE Healthcare, 27-4710-01) was incubated for 1 h. Two washes preceded 1-h incubation with goat anti-mouse-HRP antibody (1:8000, Jackson ImmunoResearch Laboratories, 115-035-174). After two final wash steps, 70 μl of 3,3′,5,5′-tetramethylbenzidine substrate (Thermo Scientific) was added/well at room temperature. The colorimetric reaction was performed at 30 °C and 700 rpm for 3–5 min and stopped with 70 μl of 0.15 M H_2SO_4/well. The optical density was read at 450-nm wavelength with a Molecular Devices plate reader. Inhibition curves were fitted with Prism® software.

HPLC-based Activity Profiling of Extracts—HPLC-based activity profiling was performed on a Waters 2695 Alliance separation module equipped with a Waters 996 photodiode array detector and a C18 SunFire column (3.0 × 150 mm, 3.5 μm). The mobile phase consisted of 0.1% formic acid in H_2O (A) and MeCN (B). A gradient of 5–100% B in 30 min was applied. The flow rate was 0.4 ml/min. 900 μg of extract was injected in three portions, and time-based microfractions were collected into a deep-well 96-well microtiter plate (29 fractions of 60 s each) with a Gilson FC204. The microtiter plate was dried in a Genevac EZ-2 evaporating system at 35 °C overnight. The dried fractions were taken up in 16 μl of DMSO, and 2 μl was used in the CUG_{78}-MBNL1 inhibition assay.

Myoblast Splicing Assay—Two human fibroblast cell lines with a doxycycline-inducible MyoD construct for differentiation into myoblasts were kindly provided by Denis Furling (Université Pierre et Marie Curie-Paris, Paris, France) (31). The WT control cell line was derived from a 19-year-old healthy individual with a normal CTG repeat length in the DMPK locus, whereas the DM1 cell line was derived from an 11-year-old individual with a CTG_{1300} repeat length in the same locus. Fibroblasts were grown in growth medium (GM; 1× DMEM with 1× GlutaMax, 10% FBS (Gibco), 30 mM HEPES, and 50 μg/ml gentamycin (Sigma)) at 37 °C under 5% CO_2. 50,000 cells/well were seeded in 6-well plates and grown for 3 days. Cells were washed with 1× DMEM, and then differentiation medium (GM with 5 μg/ml doxycycline) was added. After 24 h in differentiation medium, the cells were washed with 1× DMEM and treated for 24 h with either compound or DMSO in differentiation medium. The cells were washed with 1× PBS, and total RNA was extracted with TRI reagent (Sigma) according to the protocol of the manufacturer. 500 ng of RNA was used for reverse transcription with the SuperScript III first-strand synthesis system for RT-RCR (Invitrogen), according to the protocol of the manufacturer with random hexamer primers. Pre-mRNA targets were chosen based on prior studies of small molecules in cellular and *in vivo* models of DM1 (21). 1 μl of cDNA was used for qPCR with 40 amplification cycles of 15 s at 95 °C, 15 s at 61 °C, and 20 s at 72 °C. qPCR was performed with two primer pairs, one primer pair only amplifying splicing variants that contain an investigated alternative exon and the other primer pair amplifying all possible splicing variants (pan): *INSR*, 5′GACCTGGTCTCCACCATTCG3′ (forward), 5′CACCAGTGCCTGAAGAGGTT3′ (reverse exon), and 5′ACGAAAACCACGTTGTGCAG3′ (reverse pan); *TNNT2*, 5′CAGCTGCTGTTCTGAGGGAG3′ (forward), 5′CTGCTCGTCTTCGTCCTCTC3′ (reverse exon), and 5′CCTCGTACTCTTCCACCACC3′ (reverse pan). *β-ACTIN* was used as a control gene with the following primers: forward, 5′CCAACCGCGAGAAGATGA3′; reverse, 5′CCAGAGGCGTACAGGGATAG3′. MBNL1-independent splicing of *ATE1* and *FHL1* (33) was analyzed using the following primers: *ATE1*, 5′GGGTTTCCAGGCTCAAGGTC3′ (forward), 5′TGAACTGCGAACTTGGTGGA3′ (reverse exon), and 5′TGTGTGATGCATTCTCTGGTAA3′ (reverse pan); *FHL1*, 5′ATGCCGATTGCTTTGTGTGT3′ (forward), 5′CTGGGTGGCTCACTCTTGAC3′ (reverse exon), and 5′TCTTGCATCCAGCACACTTCT3′ (reverse pan). Amplification was done with HOT FIREPol EvaGreen qPCR mixture (Solis BioDyne) on an Applied Biosystems StepOnePlus real-time PCR machine. The amount of the splicing variant, including the investigated

alternative exon, was quantified relative to the amount of the pan-amplicon, which gave a percentage of exon inclusion.

For classical RT-PCR, 1 μl of cDNA was used for PCR with 40 amplification cycles of 15 s at 95 °C, 15 s at 61 °C, and 20 s at 72 °C. The following primer pairs were used: *INSR*, 5′CCAAAGACAGACTCTCAGAT3′ (forward) and 5′AACATCGCCAAGGGACCTGC3′ (reverse); *TNNT2*, 5′ATAGAAGAGGTGGTGGAAGAGTAC3′ (forward) and 5′GTCTCAGCCTCTGCTTCAGCATCC3′ (reverse). Amplification was done with HOT Start DNA polymerase (Solis BioDyne) on an Applied Biosystems PCR machine. The PCR products were run on 3% agarose gels stained with RedSafe (iNtRON). Gels were imaged with a Gel Doc XR+ (Bio-Rad).

Myoblast Viability Assay—C2C12 mouse myoblasts were plated in 96-well plates in GM (4000 cells/well, 100 μl/well) and grown overnight. Compounds/DMSO were then added in GM. After incubation for 48 h, the CellTiter-Blue® reagent (Promega) was added according to the protocol of the manufacturer. Fluorescence was measured with an Infinite F500 plate reader (Tecan) with an excitation/emission wavelength of 535/590 nm. Signal concentration curves were fitted with Prism® software to determine toxicity IC_{50} values.

FISH and Immunofluorescence—15,000 fibroblasts/well were grown for 24 h in GM on 0.3% gelatin-coated coverslips (24-well dishes). Cells were washed with 1× DMEM and differentiated in DM for 24 h. Washing with 1× DMEM preceded the compound/vehicle incubation in DM for 24 h. Coverslip washing, permeabilization of myoblasts, FISH and immunostaining with MBNL1 antibody (A2764, a kind gift from Charles Thornton, University of Rochester) was performed according to the procedure of Warf *et al.* (21). Wash buffer I contained 1× PBS and 0.05% Triton X-100. Coverslips were blocked in buffer (wash buffer I and 3% BSA, 15 min, room temperature) before MBNL1 antibody incubation. 1:750 diluted goat anti-rabbit DyLight 488 antibody (Jackson ImmunoResearch Laboratories, 111-485-144) was added in wash buffer I (1 h, room temperature). Myoblasts were stained with 1:20,000 DAPI in wash buffer I (5 min, room temperature). Coverslips were mounted on glass slides with FluorSave reagent (Calbiochem). Cells were imaged using a Leica DMRE fluorescence microscope. For quantification, the amount of foci was counted for 3 × 50 randomly chosen nuclei from three experiments.

Treatment of Mice—HSA^{LR} transgenic mice in line 20b were kindly provided by C. Thornton. FVB/N (WT) control mice were obtained from the animal facility of the Department of Biomedicine, University Hospital Basel, Switzerland. Age- and gender-matched groups of a minimum of three mice (10–12 weeks old, male) of WT or HSA^{LR} mice were treated by two intraperitoneal injections of compound/vehicle (12-h interval). Harmine hydrochloride was administered in saline and berberine chloride, dihydroberberine, and palmatine chloride hydrate in 5% DMSO/PBS. Mice were sacrificed 2–4 h after the second injection. Dissected quadriceps muscle was powdered after freezing in liquid nitrogen. Animal studies were conducted in accordance with the Animal Research Authorities (Canton Basel-Stadt, Switzerland, permit no. 2632).

Mouse Skeletal Muscle Splicing Assay—Powdered quadriceps muscle tissue was taken up in TRI reagent (Sigma) and was grinded with a Polytron® (Kinematica) for 30 s at 4 °C. Insoluble material was removed by centrifugation at 12,000 rpm (10 min, 4 °C). From the supernatant, RNA was extracted with TRI reagent (Sigma) according to the protocol of the manufacturer. The qPCR amplification protocol was analogous to the myoblast qPCR protocol with the following primer pairs: CLCN1, 5′GGGCGTGGGATGCTACTTTG3′ (forward exon), 5′CTGACATCCTGACAGTGGGC3′ (forward pan), and 5′AGGACACGGAACACAAAGGC3′ (reverse); SERCA1, 5′GCCCTGGACTTTACCCAGTG3′ (forward), 5′ACGGTTCAAAGACATGGAGGA3′ (reverse exon), and 5′CCTCCAGATAGTTCCGAGCA3′ (reverse pan). Pre-mRNA targets were chosen based on prior studies of small molecules in cellular and *in vivo* models of DM1 (21). Classical RT-PCR was performed analogously to the myoblast splicing assay with the following primers: CLCN1, 5′GGAATACCTCACACTCAAGGCC3′ (forward) and 5′CACGGAACACAAAGGCACTGAATGT3′ (reverse); SERCA1, 5′GCTCATGGTCCTCAAGATCTCAC3′ (forward) and 5′GGGTCAGTGCCTCAGCTTTG3′ (reverse).

Western Blotting Detection of CLCN1 Protein from Mouse Skeletal Muscle—Proteins were extracted from powdered mouse quadriceps muscle according to Dimauro *et al.* (45) to obtain the nuclear/membrane fraction. Instead of NET, radioimmunoprecipitation assay+ buffer (50 mM Tris HCL (pH 8.0), 150 mM NaCl, 1% Nonidet P-40, 0.5% sodium deoxycholate, 1% Triton X-100, 0.1% SDS, and 10% glycerol) was used, containing protease and phosphatase inhibitor tablets (Roche). Protein concentrations were determined with a BCA assay (Sigma). 10-μg samples were separated by Tris/glycine SDS-PAGE on 8% gels and analyzed by Western blotting using Protran BA85 nitrocellulose membranes (GE Healthcare), rabbit polyclonal antibody against the N terminus of full-length CLCN1 (1:1000, a kind gift from Thomas Cooper, Baylor College of Medicine) (13), and HRP-tagged goat anti-rabbit secondary antibody (1:10000, Jackson ImmunoResearch Laboratories, 111-035-003). To detect lamin B (loading control), goat polyclonal anti-lamin B antibody (1:1000, Santa Cruz Biotechnology, sc-6216) and HRP-tagged swine anti-goat antibody (1:10,000, Life Technologies, ACI3404) were used. All antibodies were incubated in 1× TBS, 3% BSA, 0.1% Tween 20, and 0.08% SDS. Membranes were incubated for 5 min with LumiGLO (KPL) chemiluminescent substrate and exposed to Super RX films (Fuji).

Western Blotting Detection of MBNL1 Protein from Myoblasts—Human fibroblasts were cultured, differentiated into myoblasts, and treated in 6-well plates as described above for the myoblast splicing assay. Myoblasts were washed with 1× PBS, harvested in 1× PBS, and centrifuged for 10 min at 4 °C and 15,000 rpm, and then the pellet was resuspended in 100 μl of radioimmune precipitation assay+ buffer containing protease and phosphatase inhibitor tablets (Roche). After 2-h incubation on a wheel at 4 °C, the samples were centrifuged for 10 min at 4 °C and 12,000 rpm. Protein concentrations in supernatants were determined with a BCA assay (Sigma). 10-μg samples were separated by Tris/glycine SDS-PAGE on 12% gels. Western blotting was performed as described above using 1:5000 diluted A2764 anti-MBNL1 antibody and anti-rabbit

secondary antibody (1:10,000, Jackson ImmunoResearch Laboratories, 111-035-003).

Histological Analysis of Internalized Nuclei—8-μm cryostat cross-sections from gastrocnemius mouse muscle were stained with H&E and analyzed for the percentage of muscle fibers with internalized nuclei.

Author Contributions—R. H. conducted the screening, the splicing and focus evaluation, as well as the *in vivo* experiments. He obtained part of the funding, analyzed the results, and wrote the paper. M. T. F. performed the workup of the plant and fungus extracts, including their chemical analysis, and participated in writing of the paper. J. K. established MBNL1 protein expression and purification and supervised the experiments. F. K. and A. S. provided technical assistance. B. E. and T. W. performed the histological analysis of mouse skeletal muscle. M. S. conceived the idea for this project, secured funding, and supervised the project. O. P. and M. H. established the natural product library and profiling approach and supervised the characterization of natural products.

Acknowledgments—We thank D. Furling and the platform for immortalization of human cells from the Institut de Myologie (Paris, France) for the DM1 and control fibroblast cell lines, T. Cooper for the CLCN1 antibody, M. Swanson for the MBNL1 cDNA, and C. Thornton for the HSA^{LR} mice and the MBNL1 antibody.

References

1. Machuca-Tzili, L., Brook, D., and Hilton-Jones, D. (2005) Clinical and molecular aspects of the myotonic dystrophies: a review. *Muscle Nerve* **32,** 1–18
2. Mahadevan, M., Tsilfidis, C., Sabourin, L., Shutler, G., Amemiya, C., Jansen, G., Neville, C., Narang, M., Barceló, J., and O'Hoy, K. (1992) Myotonic-dystrophy mutation: an unstable CTG repeat in the 3′ untranslated region of the gene. *Science* **255,** 1253–1255
3. Brook, J. D., McCurrach, M. E., Harley, H. G., Buckler, A. J., Church, D., Aburatani, H., Hunter, K., Stanton, V. P., Thirion, J. P., and Hudson, T. (1992) Molecular basis of myotonic dystrophy: expansion of a trinucleotide (CTG) repeat at the 3′ end of a transcript encoding a protein kinase family member. *Cell* **69,** 385–385
4. Mankodi, A., Logigian, E., Callahan, L., McClain, C., White, R., Henderson, D., Krym, M., and Thornton, C. A. (2000) Myotonic dystrophy in transgenic mice expressing an expanded CUG repeat. *Science* **289,** 1769–1773
5. Wheeler, T. M., Sobczak, K., Lueck, J. D., Osborne, R. J., Lin, X., Dirksen, R. T., and Thornton, C. A. (2009) Reversal of RNA dominance by displacement of protein sequestered on triplet repeat RNA. *Science* **325,** 336–339
6. Taneja, K. L., McCurrach, M., Schalling, M., Housman, D., and Singer, R. H. (1995) Foci of trinucleotide repeat transcripts in nuclei of myotonic-dystrophy cells and tissues. *J. Cell Biol.* **128,** 995–1002
7. Davis, B. M., McCurrach, M. E., Taneja, K. L., Singer, R. H., and Housman, D. E. (1997) Expansion of a CUG trinucleotide repeat in the 3′ untranslated region of myotonic dystrophy protein kinase transcripts results in nuclear retention of transcripts. *Proc. Natl. Acad. Sci. U.S.A.* **94,** 7388–7393
8. Miller, J. W., Urbinati, C. R., Teng-Umnuay, P., Stenberg, M. G., Byrne, B. J., Thornton, C. A., and Swanson, M. S. (2000) Recruitment of human muscleblind proteins to (CUG)(n) expansions associated with myotonic dystrophy. *EMBO J.* **19,** 4439–4448
9. Yuan, Y., Compton, S. A., Sobczak, K., Stenberg, M. G., Thornton, C. A., Griffith, J. D., and Swanson, M. S. (2007) Muscleblind-like 1 interacts with RNA hairpins in splicing target and pathogenic RNAs. *Nucleic Acids Res.* **35,** 5474–5486
10. Philips, A. V., Timchenko, L. T., and Cooper, T. A. (1998) Disruption of splicing regulated by a CUG-binding protein in myotonic dystrophy. *Science* **280,** 737–741
11. Lin, X., Miller, J. W., Mankodi, A., Kanadia, R. N., Yuan, Y., Moxley, R. T., Swanson, M. S., and Thornton, C. A. (2006) Failure of MBNL1-dependent post-natal splicing transitions in myotonic dystrophy. *Hum. Mol. Genet.* **15,** 2087–2097
12. Mankodi, A., Takahashi, M. P., Jiang, H., Beck, C. L., Bowers, W. J., Moxley, R. T., Cannon, S. C., and Thornton, C. A. (2002) Expanded CUG repeats trigger aberrant splicing of ClC-1 chloride channel pre-mRNA and hyperexcitability of skeletal muscle in myotonic dystrophy. *Mol. Cell* **10,** 35–44
13. Charlet-B, N., Savkur, R. S., Singh, G., Philips, A. V., Grice, E. A., and Cooper, T. A. (2002) Loss of the muscle-specific chloride channel in type 1 myotonic dystrophy due to misregulated alternative splicing. *Mol. Cell* **10,** 45–53
14. Savkur, R. S., Philips, A. V., and Cooper, T. A. (2001) Aberrant regulation of insulin receptor alternative splicing is associated with insulin resistance in myotonic dystrophy. *Nat. Genet.* **29,** 40–47
15. Hino, S., Kondo, S., Sekiya, H., Saito, A., Kanemoto, S., Murakami, T., Chihara, K., Aoki, Y., Nakamori, M., Takahashi, M. P., and Imaizumi, K. (2007) Molecular mechanisms responsible for aberrant splicing of SERCA1 in myotonic dystrophy type 1. *Hum. Mol. Genet.* **16,** 2834–2843
16. Ho, T. H., Charlet-B, N., Poulos, M. G., Singh, G., Swanson, M. S., and Cooper, T. A. (2004) Muscleblind proteins regulate alternative splicing. *EMBO J.* **23,** 3103–3112
17. Berg, J., Jiang, H., Thornton, C. A., and Cannon, S. C. (2004) Truncated ClC-1 mRNA in myotonic dystrophy exerts a dominant-negative effect on the Cl current. *Neurology* **63,** 2371–2375
18. Krzyzosiak, W. J., Sobczak, K., Wojciechowska, M., Fiszer, A., Mykowska, A., and Kozlowski, P. (2012) Triplet repeat RNA structure and its role as pathogenic agent and therapeutic target. *Nucleic Acids Res.* **40,** 11–26
19. Lee, J. E., Bennett, C. F., and Cooper, T. A. (2012) RNase H-mediated degradation of toxic RNA in myotonic dystrophy type 1. *Proc. Natl. Acad. Sci. U.S.A.* **109,** 4221–4226
20. Kanadia, R. N., Shin, J., Yuan, Y., Beattie, S. G., Wheeler, T. M., Thornton, C. A., and Swanson, M. S. (2006) Reversal of RNA missplicing and myotonia after muscleblind overexpression in a mouse poly(CUG) model for myotonic dystrophy. *Proc. Natl. Acad. Sci. U.S.A.* **103,** 11748–11753
21. Warf, M. B., Nakamori, M., Matthys, C. M., Thornton, C. A., and Berglund, J. A. (2009) Pentamidine reverses the splicing defects associated with myotonic dystrophy. *Proc. Natl. Acad. Sci. U.S.A.* **106,** 18551–18556
22. Arambula, J. F., Ramisetty, S. R., Baranger, A. M., and Zimmerman, S. C. (2009) A simple ligand that selectively targets CUG trinucleotide repeats and inhibits MBNL protein binding. *Proc. Natl. Acad. Sci. U.S.A.* **106,** 16068–16073
23. Pushechnikov, A., Lee, M. M., Childs-Disney, J. L., Sobczak, K., French, J. M., Thornton, C. A., and Disney, M. D. (2009) Rational design of ligands targeting triplet repeating transcripts that cause RNA dominant disease: application to myotonic muscular dystrophy type 1 and spinocerebellar ataxia type 3. *J. Am. Chem. Soc.* **131,** 9767–9779
24. Childs-Disney, J. L., Hoskins, J., Rzuczek, S. G., Thornton, C. A., and Disney, M. D. (2012) Rationally designed small molecules targeting the RNA that causes myotonic dystrophy type 1 are potently bioactive. *ACS Chem. Biol.* **7,** 856–862
25. Gareiss, P. C., Sobczak, K., McNaughton, B. R., Palde, P. B., Thornton, C. A., and Miller, B. L. (2008) Dynamic combinatorial selection of molecules capable of inhibiting the (CUG) repeat RNA-MBNL1 interaction *in vitro*: discovery of lead compounds targeting myotonic dystrophy (DM1). *J. Am. Chem. Soc.* **130,** 16254–16261
26. Ofori, L. O., Hoskins, J., Nakamori, M., Thornton, C. A., and Miller, B. L. (2012) From dynamic combinatorial "hit" to lead: *in vitro* and *in vivo* activity of compounds targeting the pathogenic RNAs that cause myotonic dystrophy. *Nucleic Acids Res.* **40,** 6380–6390
27. Hoskins, J. W., Ofori, L. O., Chen, C. Z., Kumar, A., Sobczak, K., Nakamori, M., Southall, N., Patnaik, S., Marugan, J. J., Zheng, W., Austin, C. P., Disney, M. D., Miller, B. L., and Thornton, C. A. (2014) Lomofungin and dilomofungin: inhibitors of MBNL1-CUG RNA binding with distinct cellular effects. *Nucleic Acids Res.* **42,** 6591–6602
28. Chen, C. Z., Sobczak, K., Hoskins, J., Southall, N., Marugan, J. J., Zheng, W., Thornton, C. A., and Austin, C. P. (2012) Two high-throughput

screening assays for aberrant RNA-protein interactions in myotonic dystrophy type 1. *Anal. Bioanal. Chem.* **402,** 1889–1898
29. Koehn, F. E., and Carter, G. T. (2005) The evolving role of natural products in drug discovery. *Nat. Rev. Drug Discov.* **4,** 206–220
30. Wilson, D. N. (2014) Ribosome-targeting antibiotics and mechanisms of bacterial resistance. *Nat. Rev. Microbiol.* **12,** 35–48
31. Chaouch, S., Mouly, V., Goyenvalle, A., Vulin, A., Mamchaoui, K., Negroni, E., Di Santo, J., Butler-Browne, G., Torrente, Y., Garcia, L., and Furling, D. (2009) Immortalized skin fibroblasts expressing conditional MyoD as a renewable and reliable source of converted human muscle cells to assess therapeutic strategies for muscular dystrophies: validation of an exon-skipping approach to restore dystrophin in Duchenne muscular dystrophy cells. *Hum. Gene Ther.* **20,** 784–790
32. Potterat, O., and Hamburger, M. (2014) Combined use of extract libraries and HPLC-based activity profiling for lead discovery: potential, challenges, and practical considerations. *Planta Med.* **80,** 1171–1181
33. Mykowska, A., Sobczak, K., Wojciechowska, M., Kozlowski, P., and Krzyzosiak, W. J. (2011) CAG repeats mimic CUG repeats in the misregulation of alternative splicing. *Nucleic Acids Res.* **39,** 8938–8951
34. Kumar, G. S. (2012) RNA targeting by small molecules: binding of protoberberine, benzophenanthridine and *Aristolochia* alkaloids to various RNA structures. *J. Biosci.* **37,** 539–552
35. Nafisi, S., Malekabady, Z. M., and Khalilzadeh, M. A. (2010) Interaction of β-carboline alkaloids with RNA. *DNA Cell Biol.* **29,** 753–761
36. Islam, M. M., Chowdhury, S. R., and Kumar, G. S. (2009) Spectroscopic and calorimetric studies on the binding of alkaloids berberine, palmatine and coralyne to double stranded RNA polynucleotides. *J. Phys. Chem. B* **113,** 1210–1224
37. Cetinkol, O. P., and Hud, N. V. (2009) Molecular recognition of poly(A) by small ligands: an alternative method of analysis reveals nanomolar, cooperative and shape-selective binding. *Nucleic Acids Res.* **37,** 611–621
38. Thomas, J. R., and Hergenrother, P. J. (2008) Targeting RNA with small molecules. *Chem. Rev.* **108,** 1171–1224
39. Warf, M. B., and Berglund, J. A. (2007) MBNL binds similar RNA structures in the CUG repeats of myotonic dystrophy and its pre-mRNA substrate cardiac troponin T. *RNA* **13,** 2238–2251
40. Turner, N., Li, J.-Y., Gosby, A., To, S. W., Cheng, Z., Miyoshi, H., Taketo, M. M., Cooney, G. J., Kraegen, E. W., James, D. E., Hu, L.-H., Li, J., and Ye, J.-M. (2008) Berberine and its more biologically available derivative, dihydroberberine, inhibit mitochondrial respiratory complex I: a mechanism for the action of berberine to activate AMP-activated protein kinase and improve insulin action. *Diabetes* **57,** 1414–1418
41. Jiang, J.-F., Wang, Y.-G., Hu, J., Lei, F., Kheir, M. M., Wang, X.-P., Chai, Y.-S., Yuan, Z.-Y., Lu, X., Xing, D.-M., Du, F., and Du, L.-J. (2013) Novel effect of berberine on thermoregulation in mice model induced by hot and cold environmental stimulation. *PLoS ONE* 10.1371/journal.pone.0054234
42. Guan, Y. B., Louis, E. D., and Zheng, W. (2001) Toxicokinetics of tremorogenic natural products, harmane and harmine, in male Sprague-Dawley rats. *J. Toxicol. Env. Health A* **64,** 645–660
43. Lee, S. S., Kai, M., and Lee, M. K. (1999) Effects of natural isoquinoline alkaloids on monoamine oxidase activity in mouse brain: inhibition by berberine and palmatine. *Med. Sci. Res.* **27,** 749–751
44. Herraiz, T., González, D., Ancín-Azpilicueta, C., Arán, V. J., and Guillén, H. (2010) β-Carboline alkaloids in *Peganum harmala* and inhibition of human monoamine oxidase (MAO). *Food Chem. Toxicol.* **48,** 839–845
45. Dimauro, I., Pearson, T., Caporossi, D., and Jackson, M. J. (2012) A simple protocol for the subcellular fractionation of skeletal muscle cells and tissue. *BMC Res. Notes* **5,** 513–513

Identification of Plant-derived Alkaloids with Therapeutic Potential for Myotonic Dystrophy Type I

Ruben Herrendorff, Maria Teresa Faleschini, Adeline Stiefvater, Beat Erne, Tatiana Wiktorowicz, Frances Kern, Matthias Hamburger, Olivier Potterat, Jochen Kinter and Michael Sinnreich

J. Biol. Chem. 2016, 291:17165-17177.
doi: 10.1074/jbc.M115.710616 originally published online June 13, 2016
